

Chapter 13

Formulation optimization and characterization of
Olanzapine loaded Solid lipid nanoparticles – Effect of
stabilizer on the particle size and stability

13.1 INTRODUCTION

Solid Lipid Nanoparticles are usually free from the risk of acute or chronic toxicity because they are composed of physiological and biocompatible lipids. Various lipids including triglycerides (Heiati H et al., 1998; Bunjes H et al., 1996) and hard fat waxes (Westesen K et al., 1997; Cavalli R et al., 1992) have been used for the formulation of SLN. The choice of emulsifier and co emulsifier however depends on the route of administration and is more critical in parenteral delivery (Mehnert W et al., 2001). Surfactants have been known to play a vital role in the stabilization of the colloidal particles. In addition to their stabilization properties, surfactants also play a vital role in the crystallization behavior of the lipids on storage (Bunjes H et al., 1996). The effect of lipid type on the final mean particle size of the SLN dispersions formed has also been reported by many research teams. Other factors like the velocity of lipid crystallization, the lipid hydrophilicity, influence on self-emulsifying properties on the shape of the lipid crystals, and hence the surface area were found to affect the final size of the SLN dispersions (Siekmann B et al., 1992). Till date only few attempts have been made to study the effect of the surfactant type on the nanoparticle stabilization, crystallinity changes and physical stability of the SLN dispersions.

In the previous chapter, the effect of the lipid type was studied on the entrapment of olanzapine in the lipid matrix. It was found that SLN dispersions prepared from glyceryl tristearate gave the highest entrapment among the different lipids used (Chapter 12). In this chapter, an attempt has been made to explore the effect of surfactant type in the nanoparticle stabilization, crystallinity changes and physical stability of the SLN dispersions. For this, three surfactants were selected namely Gelucire[®] 44/14 (PEG-32 glyceryl laurate), Transcutol[®] (diethylene glycol monoethyl ether), and Poloxamer 188 (co-block polymer of polyoxypropylene and polyoxyethylene). The effect of homogenization pressure and homogenization cycle number on the size of nanoparticles were determined and optimized. The nanoparticles were characterized by differential scanning calorimetry, X-ray diffraction pattern, electron microscopy and in vitro release profile was determined. Electrolyte induced flocculation test was performed to study the in vitro steric stability of the nanoparticles. Surface hydrophobicity was determined by Rose Bengal adsorption method. The nanoparticles were subjected for short term stability studies and the optimum stability conditions were determined.

13.2 MATERIALS AND METHODS

Materials

Olanzapine (OL) was received as a gift sample from Sun Pharmaceuticals, India. Poloxamer 407 was received as a free gift sample from BASF, Germany. Hydrogenated soya phosphatidyl choline (HSPC) was purchased from Lipoid GmbH (Ludwigshafen, Germany). Glyceryl tristearate (tri glyceride derivative of 16 carbon fatty acid stearic acid and glycerol) was kindly provided by Sasol Chemicals, Germany. Transcutol[®] and Gelucire[®] 44/14 was obtained as a gift sample from Gattefosse, France. Poloxamer 188 was received as a free gift sample from BASF, USA. All other chemicals used in the study were of analytical grade. Water used in all the studies was distilled and filtered through 0.22 µm nylon filter before use.

Methods

Preparation and optimization of Solid Lipid Nanoparticles

Solid lipid nanoparticles (SLNs) were prepared by the slight modification of melt emulsification and high pressure homogenization method reported earlier (Reddy et al., 2006). Briefly, the lipid was melted and OL was dissolved to obtain drug-lipid mixture. Hydrogenated soya phosphatidyl choline (HSPC) was dissolved in about 0.3 ml chloroform and added to the above lipid- drug mixture. The mixture was warmed at about 60 to 65°C to evaporate the chloroform totally and the clear lipid melt containing HSPC was added to the hot aqueous surfactant solution (2% poloxamer 188 incase of POL188 SLN; 5% Transcutol[®] incase of TROL SLN; 2% Gelucire[®] 44/14 incase of GOL SLN) preheated to 10°C above the melting point of the lipid, under high shear homogenization at 9500 rpm for 1 minute using Ultra Turrax (Ultra Turrax T-25, Germany) to result in a crude emulsion. The crude emulsion was subsequently homogenized in a high pressure homogenizer (Emulsiflex C5, Avestin, Canada) in a water bath maintained at 10°C above the melting point of the lipid. The nanoemulsion obtained was then cooled at room temperature to recrystallize the lipid back to the solid state. This resulted in the formation of drug entrapped SLN dispersions in an aqueous media.

The SLN dispersions had a lipid content of 5%; the effect of the homogenization pressure, homogenization cycle number and the surfactant concentration on the mean particle size of the nanoparticles formed was studied. To study the entrapment efficiency the OL content with respect to the lipid matrix was varied from 2 to 5%.

Estimation of olanzapine in SLNs

The SLN in dispersion was aggregated by adding 0.1 mL of 10 mg/mL protamine sulfate solution, and the dispersion was centrifuged at 8000 rpm (Remi cooling centrifuge, Mumbai, India) to obtain the pellet. 0.1 ml of the supernatant was diluted suitably with 0.1N HCl and the free drug content was determined in a UV-visible spectrophotometer (Shimadzu, Japan) at 258 nm against suitable solvent blank. The pellet obtained was washed with distilled water and lyophilized after the addition of 2 parts by weight mannitol with respect to total lipid content of the formulation. Accurately weighed lyophilized powder was dissolved in a mixture of methanol-chloroform (1:1); and suitably diluted with the same solvent mixture and analyzed in a UV-visible spectrophotometer (Shimadzu, Japan) at 276 nm against suitable solvent blank.

Characterization of SLN

A. Particle size and zeta potential measurements

Size and zeta potential of the SLN dispersions were measured by photon correlation spectroscopy (PCS) using Malvern Zetasizer Nano ZS (Malvern Instruments, UK). Size and zeta potential measurements were carried for both initial SLN dispersions and stability samples of SLN dispersions after appropriate dilution with distilled water.

B. Transmission Electron Microscopy (TEM)

TEM studies were performed in transmission electron microscope (Philips Morgagni 268). Nanoparticles were dispersed in de ionized water and one drop of the reconstituted nanoparticles was incubated on 200 – mesh carbon coated copper grid. The copper grid was fixed into sample holder and placed in vacuum chamber of the transmission electron microscope and observed under low vacuum (10^{-3} torr)

C. Differential Scanning Calorimetry (DSC)

DSC analysis was carried out using a Differential scanning calorimeter (DSC-60, Shimadzu, Japan) at a heating rate of 10°C per minute in the range of 30°C to 250°C under inert nitrogen atmosphere at a flow rate of 80ml/min. DSC thermograms were recorded for OL, bulk GTS, POL188 SLN, TROL SLN and GOL SLN are shown in figure 13.5.

D. X ray diffraction studies

Powder X-ray diffraction patterns were obtained using an X-ray diffractometer (Philips PW 1710) with Cu K α radiation generated at 30 mA and 40 kV. XRD diffraction patterns of OL, bulk GTS, POL188 SLN, TROL SLN and GOL SLN are shown in figure 13.6.

E. Determination of in vitro steric stability by electrolyte induced flocculation test

The electrolyte induced flocculation test was performed for the all the three SLN dispersions stabilized with the different stabilizers. The effect of the stabilizer to resist electrolyte induced flocculation was investigated by this test. Sodium sulphate solutions ranging from 0 M to 1.5 M were prepared in 16.7 %w/v sucrose solution (Subramanian N et al., 2003). An appropriate volume of SLN dispersion was made up to 5 ml using the sodium sulphate solutions of varying concentrations (0 M, 0.3 M, 0.6 M, 0.9 M, 1.2 M and 1.5 M) to obtain a final concentration of 1mg/ml lipid. The absorbance of the resulting dispersions was measured within 5 min at 400 nm using a UV-Visible spectrophotometer (Shimadzu, Japan) against respective blank.

F. Determination of surface hydrophobicity by Rose Bengal adsorption method

Surface hydrophobicity of the nanoparticles was evaluated by the adsorption of the hydrophobic dye Rose Bengal on the particle surface (Gessner A et al., 2000). A fixed known amount of dye was added to the nanoparticle dispersions of various concentrations. Rose Bengal undergoes partitioning between the nanoparticle surface and the dispersion medium. The SLN in dispersion were aggregated by adding 0.1 mL of 10 mg/mL protamine sulfate solution, and the dispersion was centrifuged at 8000 rpm for 10 min. The fluorescence of free dye in the supernatant was measured by the absorbance at 548nm against suitable blank. Calibration plots were constructed for the measured absorbance values against drug concentration (Table no. 13; Chapter 4). The partition co-efficient (PC) was calculated as follows,

Partition coefficient (PC) = Amount of Rose Bengal bound on the surface / amount of Rose Bengal in the dispersion medium.

PC values obtained from the above formula for each nanoparticle concentration was then plotted against the total surface area (in $\mu\text{m}^2/\text{ml}$) of the nanoparticles. The slopes of the straight lines obtained were taken as a measure of the surface hydrophobicity.

G. Stability studies - Effect of temperature

Short-term stability studies were conducted on the various OL loaded SLN dispersions for a period of six months. The initial particle size and zeta potential of the OL loaded SLN dispersions were measured immediately after high pressure homogenization using Zetasizer (Malvern Zetasizer Nano ZS). Then the batch was stored in transparent colorless glass vials (USP type I) sealed and wrapped with black paper under different temperature conditions of 4°C (in a refrigerator) and 40°C (temperature regulated oven). Samples were withdrawn after 30, 60, 90, 180 days and were subjected to particle size and zeta potential measurements.

H. In vitro drug release

In vitro release of OL from the POL188 SLN, TROL SLN and GOL SLN were determined in both 0.1 N HCl and pH 7.4 PB. OL is freely soluble in 0.1 N HCl. In vitro drug release studies for all the four SLN dispersions upto 18 hours in 0.1 N HCl and 72 hours in PH 7.4 PB. The SLN dispersion was placed in a dialysis bag (cutoff molecular weight of 12000 Daltons, Himedia, India) and sealed at both ends. The dialysis bag was then dipped into the receptor compartment containing the dissolution medium. The release of OL from solution form in pH 7.4 PB containing 1% methanol (as control) through the dialysis bag was also studied using the same media. The dissolution media was continuously stirred at 100 rpm and maintained at $37 \pm 2^\circ\text{C}$. Samples were withdrawn at regular time intervals and the same volume was replaced with fresh dissolution medium. Samples withdrawn from 0.1N HCl were analyzed spectrophotometrically at 258 nm for OL content against a solvent blank. Samples withdrawn from pH 7.4 PB were analyzed spectrophotometrically at 260 nm for OL content against a solvent blank. All experiments were repeated thrice and the average values were taken.

13.3 RESULTS AND DISCUSSION

Influence of homogenization pressure and homogenization cycle number

The optimum homogenization pressure was determined by passing the crude emulsion at different homogenization pressures such as 5000 to 10000 psi using 2% poloxamer 188 as the surfactant for POL188 SLN, 5% Transcutol® as the surfactant for TROL SLN and 2% Gelucire® 44/14 as the surfactant for GOL SLN.

As the homogenization pressure was increased from 5000 psi to 10000 psi, a decrease in mean particle diameter of SLN dispersions was observed. The optimum homogenization pressure was found to be 10000 psi for all the four lipids. Homogenization pressures above 10000 psi did not result in a significant decrease in the mean particle size diameter of the SLN dispersions. Thus 10000 psi was considered as the optimum homogenization pressure. This reduction in particle size is mainly due to the development of cavitation forces in the homogenization gap, which results in diminution of the lipid droplets to the nano size (Muller RH and Keck CM., 2004). The effect of the different homogenization pressures on the mean particle size diameter of the SLN dispersion is shown in figure 13.2.

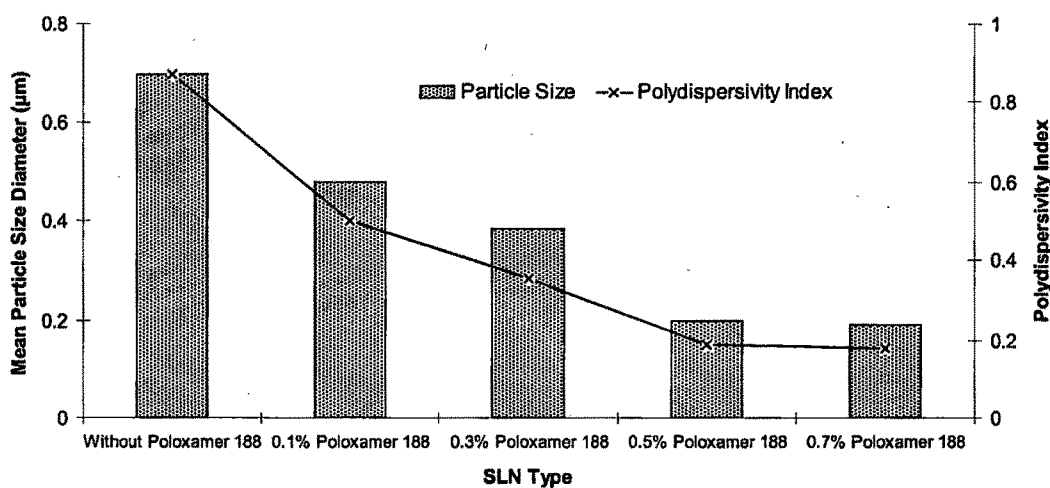


Figure 13.1: Effect of the addition of Poloxamer 188 on the mean particle size diameter and polydispersity index of TROL SLN. (Homogenization Pressure: 10000 psi; Homogenization Cycle number: 3)

In case of TROL SLN, a small modification was done. In case of the SLN dispersions prepared with only 5% Transcutol[®], there was a formation of higher amount of microparticles. Hence, 0.5% of poloxamer 188 was added to the dispersions prepared using Transcutol[®] as surfactant (Data shown in figure 13.1). SLN dispersions prepared with the combination of 0.5% poloxamer 188 as surfactant and 5% Transcutol[®] as co-surfactant were stable and is mentioned as TROL SLN from this point.

The mean particle size diameter of the nanoparticle dispersions obtained using the different surfactant concentrations mentioned above was measured after homogenizing at 10,000 psi after different homogenization cycles. It was observed that, as the number of homogenization cycles was increased, the size of SLN dispersion decreased. The size distribution curve moved towards a narrow particle size distribution upto 3 cycles and a slight increase in size was observed after the 4th cycle, accompanied by a broad size distribution. The optimum number of homogenization cycles resulting in smaller sized nanoparticles was 3 cycles. The effect of the homogenization cycle number on the mean particle size diameter of the SLN dispersion is shown in figure 13.3.

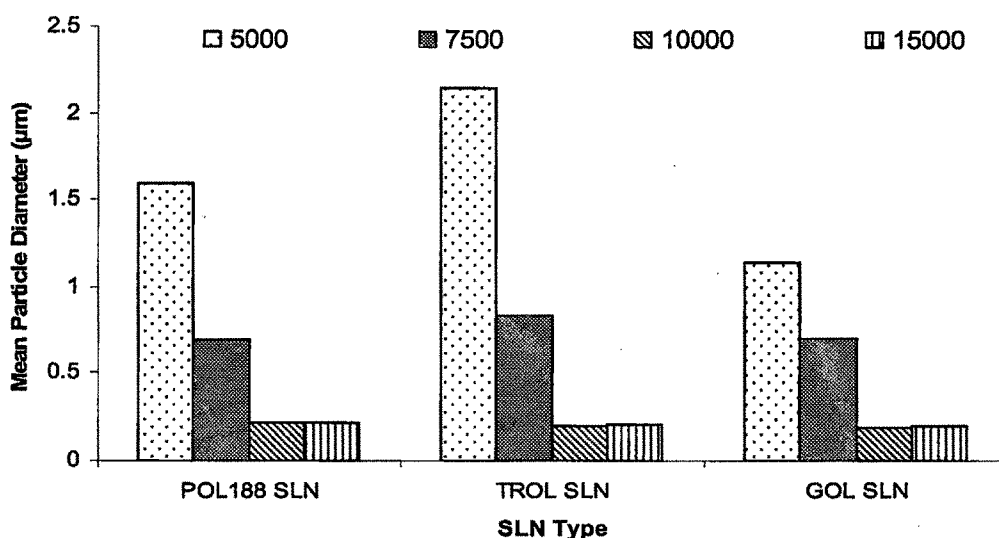


Figure 13.2: Effect of homogenization pressure on the size of solid lipid nanoparticles homogenized for three cycles

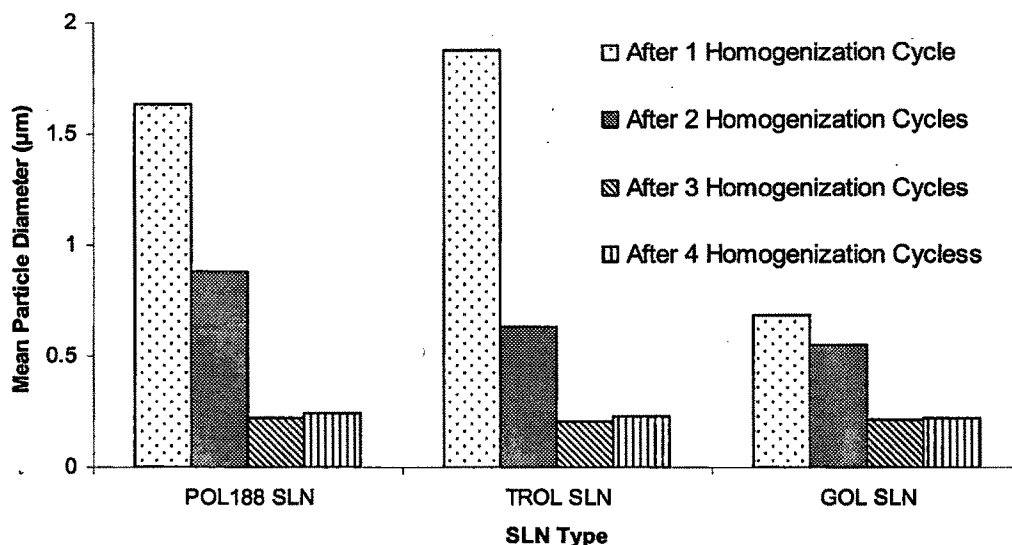


FIGURE 13.3: Effect of homogenization cycles on the size of solid lipid nanoparticles homogenized at 10,000 psi.

Optimization of Surfactant concentration

Surfactant in the formulation mainly plays a vital role in the stabilization of the nanoparticles and prevents particle growth during storage. The surfactant acts by reducing the surface tension at the oil – water interface. The surfactant being amphiphilic gets adsorbed at the interface with its hydrophilic part orienting towards the aqueous part and its lipophilic part orienting towards the oil part. Improper coverage of the oil droplet (in this case the nanoparticle surface) with the surfactant can lead to formation of in-stabilized nanoparticles with tendency to agglomerate on storage. Hence the concentration of surfactant required to effectively stabilize the nanoparticle dispersion is needed. In addition to its role in stabilization, surfactants have also been shown to play a role in the crystallization behavior of the lipids. Bunjes and co-workers demonstrated that the crystallization temperature of nanoparticles made from triglycerides depends on the stabilizer, which can lead to homogenous or surface heterogenous nucleation (Bunjes H et al., 1996).

The crystallization tendency of the particles increases with the length of the (saturated) hydrophobic chain of the stabilizer. The crystallization promoting effect of certain surfactants

is believed to be caused by an ordering process of the surfactant molecules in the stabilizer layer. The type of stabilizer was also found to influence the rate of the polymorphic transitions. It was found that the stabilization with ionic surfactants leads to a slower transition than stabilization with nonionic surfactants (Bunjés H et al., 1996). The choice of stabilizers is an important parameter to be considered in optimizing any nanoparticle formulation not only to control the particle size and stabilization of the dispersions but also to control the crystallization and polymorphic transitions (Bunjés H et al., 1996). The particle size and polydispersity index of the nanoparticles obtained with the various different concentrations of poloxamer 188 (in case of POL188 SLN), Transcutol® (in case of TROL SLN) and Gelucire® 44/14 (in case of GOL SLN) is shown in table 13.1, 13.2 and 13.3 respectively.

Parameter	0.5% w/v	1.0% w/v	1.5% w/v	2.0% w/v	2.5% w/v
	Poloxamer 188	Poloxamer 188	Poloxamer 188	Poloxamer 188	Poloxamer 188
Particle Size (nm)	1058 ± 16.23	696 ± 11.02	332 ± 8.68	218 ± 6.05	210 ± 6.52
Polydispersity Index	1.130	0.897	0.547	0.186	0.190

TABLE 13.1: The mean particle diameter of the various POL188 SLN stabilized with the various concentrations of poloxamer 188

Parameter	1.0%	2.0%	3.0%	4.0%	5.0%	5.0%
	Transcutol®	Transcutol®	Transcutol®	Transcutol®	Transcutol®	Transcutol® with 0.5% poloxamer 188
Particle Size (nm)	1568 ± 15.24	1396 ±	1258 ±	1073 ±	697 ± 7.71	198 ± 4.98
Polydispersity Index	1.620	1.560	1.500	1.280	0.870	0.192

TABLE 13.2: The mean particle diameter of various TROL SLN stabilized with the various concentrations of Transcutol®. Poloxamer 188 (0.5%w/v) was added to reduce the polydispersity index.

Parameter	0.5% w/v	1.0% w/v	1.5% w/v	2.0% w/v	2.5% w/v
	Gelucire® 44/14				
Particle Size (nm)	834 ± 6.10	460 ± 5.22	272 ± 5.88	186 ± 4.66	190 ± 4.54
Polydispersity Index	0.776	0.552	0.334	0.188	0.180

TABLE 13.3: The mean particle diameter of various GOL SLN stabilized with the various concentrations of Gelucire® 44/14

Entrapment efficiency of OL in the various SLN

Four different batches of nanoparticles were prepared by keeping the lipid concentration constant at 5%w/v and varying the concentration of olanzapine between 2%w/w, 3% w/w, 4% w/w, and 5% w/w w.r.t lipid. The results showed that increase in the concentration of the drug lead to the increase in drug entrapment efficiency of the SLN dispersions. The entrapment

efficiencies obtained for different lipids with the different drug loading are tabulated in table 13.3.

The maximum drug loading possible was 4% w.r.t the lipid. Efforts to load more drug, for instance 5% lead to decrease in the entrapment efficiency. DSC and XRD studies showed the existence of drug in the lipid matrix in the amorphous state. This can be attributed to the fact that 4% drug loading led to a saturation of the lipid matrix and higher loading levels resulted in more of free drug rather than drug encapsulated inside the lipid matrix. In the present study, there was no significant difference in the entrapment efficiencies obtained with the various SLN dispersions studied. The order of entrapment was as follows: GOL SLN ($93.41 \pm 1.45\%$) > POL188 SLN ($91.35 \pm 1.27\%$) > TROL SLN ($89.67 \pm 2.06\%$).

Concentration of OL w.r.t lipid (%w/w)	Entrapment efficacy (%) \pm S.D		
	POL188 SLN	GOL SLN	TROL SLN
2	85.42 ± 1.19	89.64 ± 1.23	89.60 ± 1.60
3	88.47 ± 1.54	90.23 ± 1.74	86.57 ± 1.12
4	91.35 ± 1.27	93.41 ± 1.45	89.67 ± 2.06
5	79.36 ± 1.41	84.29 ± 1.85	76.01 ± 1.51

Table 13.4: The entrapment efficacies of the different SLN dispersions

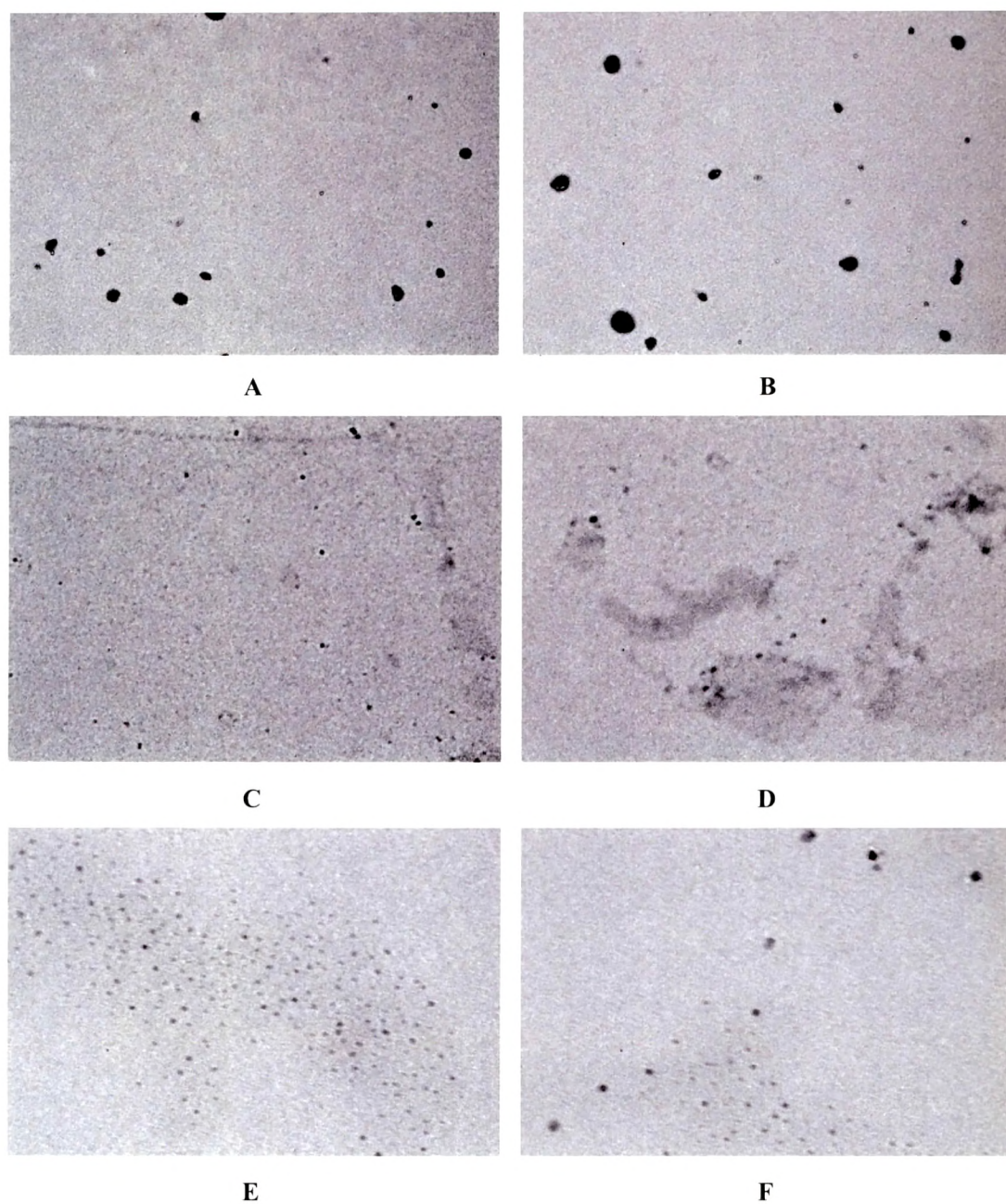


Figure 13.4: Transmission electron microscopy of GOL SLN at 44000 X (A), at 8900X (C) and at 1400 X (E); Transmission electron microscopy of TROL SLN at 44000 X (B), at 8900X (D) and at 1400 X (F);

Characterization of SLNs formulations***Differential Scanning Calorimetry (DSC)***

The crystalline structure of the nanoparticles can be assessed by differential scanning calorimetry (DSC). This is especially important when a drug exists in different polymorphic forms. The DSC results are tabulated in table 13.5. The DSC curve of OL (Figure 13.4) showed a melting endotherm at 193.05°C. This melting endotherm was not found as a sharp distinct transition in the thermograms of OL loaded GMS, PRE and WE 85 SLNs (Figure 13.5)

Reduction in the melting point (m.p.) and enthalpy of the melting endotherm of the bulk lipid was observed when formulated as SLN (table 13.5). This can be attributed to the change in crystal lattice of the lipid after incorporation of OL and formulation as nanoparticles. These results were in agreement with those observed by Freitas and co workers (Freitas C and Muller RH., 1999). They observed that the crystallization behavior of Compritol SLN differed distinctly from that of the bulk lipid. These changes were due to the increased number of lattice defects in the lipid crystal. Small particle size of the SLN means high surface energy and this creates an energetically suboptimal state which leads to a decrease in the melting point. In the present study, incorporation of OL inside the lipid matrix might have lead to an increase in the number of defects in the lipid crystal lattice leading to a decrease in m.p. of the lipid in the final SLN formulations.

Formulation	Enthalpy J/g ⁻¹	Melting Peak (°C)		
		Onset	Peak	Endset
Bulk GTS	-245.52	72.65	76.87	79.13
GOL SLN	-11.40	66.06	69.10	71.40
TROL SLN	-16.75	66.66	70.18	72.16
POL188 SLN	-26.58	68.00	71.30	73.66

Table 13.5: Differential scanning calorimetry data of bulk lipids and olanzapine loaded SLN formulations.

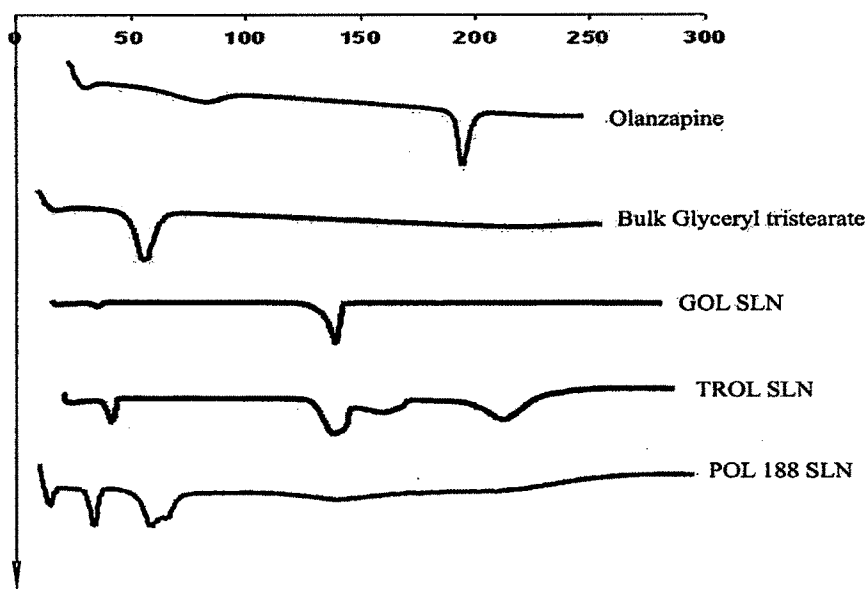


FIGURE 13.5: Differential scanning calorimetry curves of OL and the various OL loaded SLN formulations

X-ray diffraction patterns

Crystal diffraction has wide applications in the study of crystal forms (such as polymorphs, solvates, and salts). In the present study, comparison of the XRD patterns was done by considering the relative intensities of the diffracted peaks at a particular θ . The XRD data are tabulated in table 13.6. The XRD pattern of OL (Figure 13.6) shows a principal peak at angle $8.535^\circ 2\theta$; the lipid (glyceryl tristearate) shows a principal peak at $19.300^\circ 2\theta$. The principal peak of olanzapine at $8.535^\circ 2\theta$ was not observed. This shows change in the crystallinity of olanzapine after incorporation into the lipid matrix. Further, the principal peak of the lipid did not shift. However, there was a reduction in the intensity of the principal peak in all the three SLN formulations. This may be attributed to the incorporation of OL in between the crystal lattice of the lipid leading to change in the crystallinity of the OL loaded SLN. These values complement the DSC data and clearly indicate the possible change in crystallinity of the lipid after OL incorporation in to the lipid matrix.

Formulation	Peak intensity at Angle [$^{\circ}2\theta$]	
	8.535 $^{\circ}2\theta$ (Principle Peak of Olanzapine)	19.300 $^{\circ}2\theta$ (Principle Peak of Glyceryl tristearate)
Olanzapine	1011	
Glyceryl tristearate	-	2550
GOL SLN	55	557
TROL SLN	67	566
POL188 SLN	46	586

TABLE 13.6: X ray diffraction data of bulk lipids and olanzapine loaded SLN formulations.

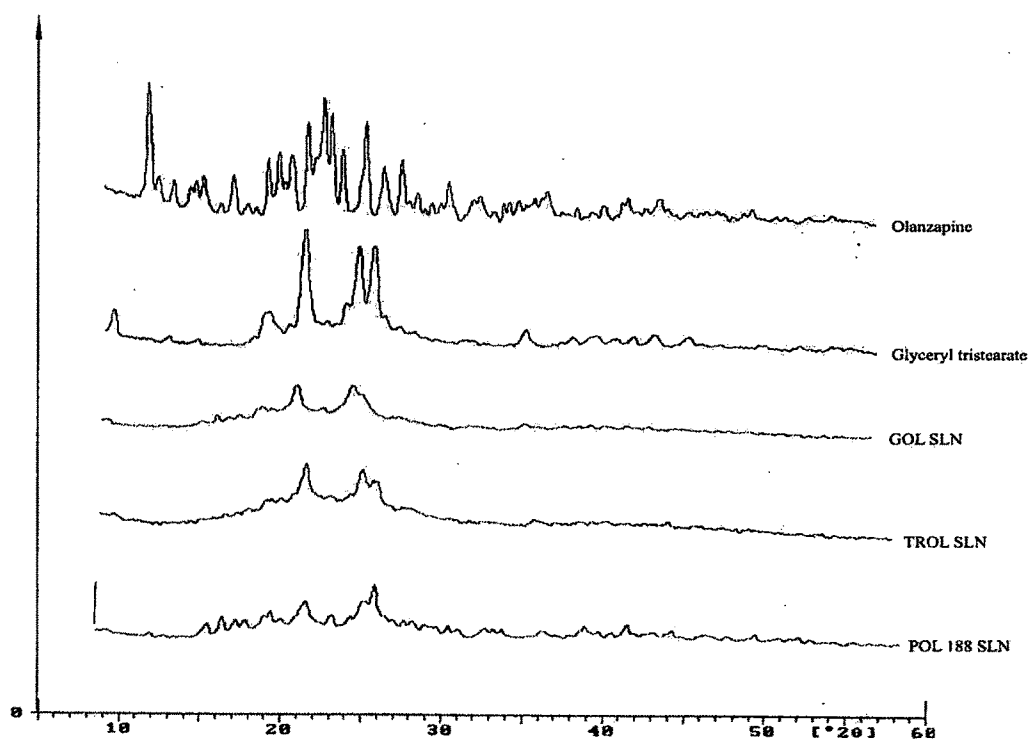


FIGURE 13.6: X – ray diffraction pattern of OL and the various OL loaded SLN formulations

Determination of in vitro steric stability by electrolyte flocculation test

The effect of the different stabilizers viz. Gelucire® 44/14, Transcutol® and poloxamer 188 on the ability of the nanoparticles to oppose electrolyte induced flocculation was investigated by this test. Coating the particulate systems with hydrophilic surfactants provide steric stability by rendering a hydrophilic surface, which in turn reduces the binding of serum opsonins and also cells of the reticuloendothelial system (Huang SK et al., 1993). Addition of electrolyte can destabilize the electrical double layer / steric stabilization provided by the stabilizer around the particle. This results in flocculation of the particles with a corresponding increase in optical turbidity of the particle dispersion which can be measured by the absorbance of the dispersion at 400nm. The scattering of the sample increased by the inverse 4th power of the wavelength of the incident light, and hence authors used a lower wavelength (400nm) was used for the measurements (Subramanian N and Murthy RSR., 2003).

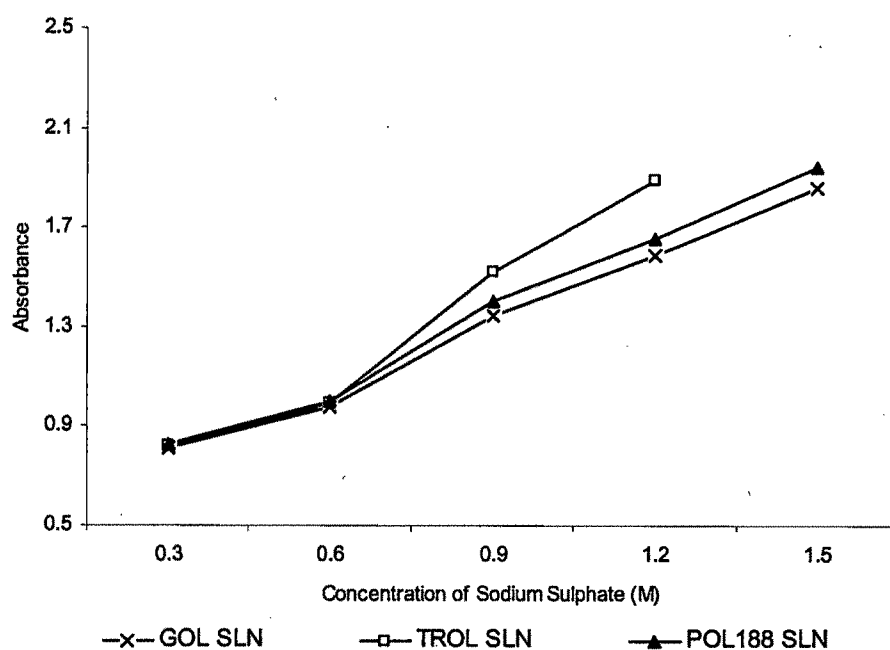


FIGURE 13.7: Steric stabilization effect of the different OL loaded SLN formulations.

In the present investigation, the nanoparticle formulations stabilized with 2.0%w/v Gelucire® 44/14, 5%w/v Transcutol® and 2.0%w/v poloxamer 188 showed a gradual increase in the flocculation as the concentration of electrolyte (sodium sulphate) was increased. All the three SLN dispersions showed signs of flocculation when the concentration of sodium sulphate was increased above 0.6M. Beyond this concentration, a sharp increase in the flocculation was observed. The results are given in figure 13.7.

Determination of surface hydrophobicity by Rose Bengal adsorption method

The slope of the straight line obtained after plotting total surface area (in $\mu\text{m}^2/\text{ml}$) of the nanoparticles and partition value obtained for Rose Bengal were used to calculate the surface hydrophobicity; steeper the slope higher the surface hydrophobicity. Results are shown in figure 13.8.

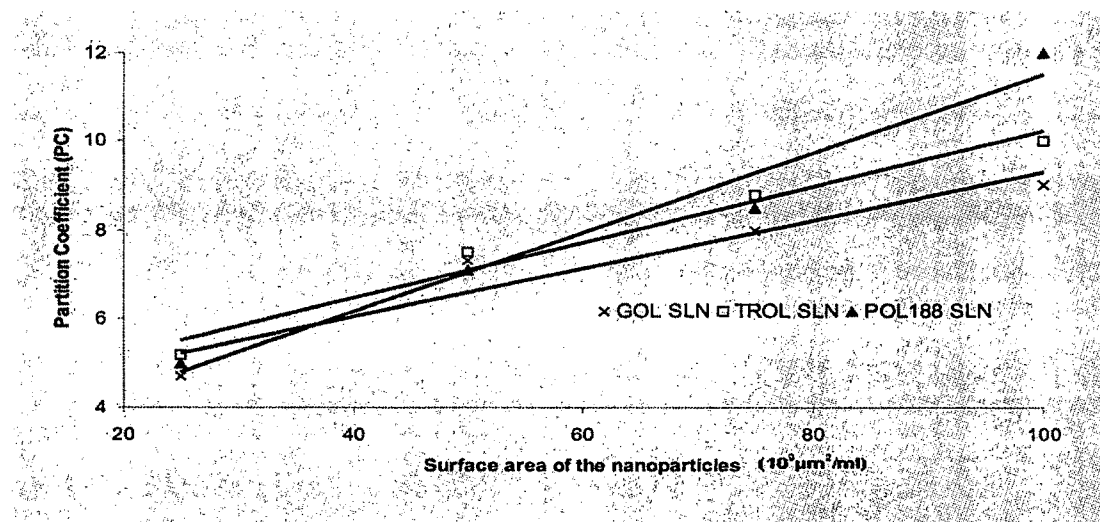


FIGURE 13.8: Plot of the partition coefficient (PC) versus the total surface area of the OL loaded nanoparticles.

The slopes i.e. the surface hydrophobicity obtained were in the order of GOL SLN (0.0896) > TROL SLN (0.0628) > POL188 SLN (0.0544). Gessner and co-workers reported that the decrease in surface hydrophobicity is accompanied with a decrease in the quantitative amount of adsorbed proteins (Gessner A et al., 2000). Qualitative changes in the protein adsorption

patterns were observed. However, they also confirmed that not only surface hydrophobicity, but also the functional groups present on the particle surface affects the protein adsorption. Gelucire® 44/14 is a mixture of glycerides and PEG 1500 esters of fatty acids. It has a melting point of 44°C and HLB value of 14. Transcutol® is hydrophilic surfactant with HLB value of 16. Carstensen and co-workers observed that the hydrophobicity of nanoparticles decreased with an increase in the polyethylene oxide chain length of the poloxamer grade used for surface stabilization (Cartensen H et al., 1991). The poloxamer block copolymers are synthetic copolymers of ethylene oxide (EO; hydrophilic part) and propylene oxide (PO; hydrophobic) with a molecular weight of around 11500. Poloxamer 188 has 74.77% of EO part (hydrophilic) and 25.23% of PO part (hydrophobic) with a HLB value of more than 24. The surface hydrophilicity values obtained were in accordance with the HLB values of the different stabilizers used. Poloxamer 188 being the hydrophilic of the three (HLB value > 24) gave SLNs with the least surface hydrophobicity (0.0544), followed by Transcutol® (HLB = 16) and Gelucire® 44/14 (HLB = 14)

Stability Studies

Effect of temperature on particle size

The particle size of the SLNs prepared from the different lipids immediately after production was not significantly different. However, their stabilities at different temperatures varied. The particle size was found to increase with storage as a result of particle aggregation. TROL SLN was found to be the most stable of the three SLN dispersions studied. Mean particle diameter of the TROL SLN stored at 40°C increased from 204 ± 5.71 nm to 522 ± 6.84 nm in six months (Figure 13.10), whereas for the TROL SLN samples stored at 4°C, increased from the initial size of 204 ± 5.71 nm to 347 ± 4.42 nm (Figure 13.9). Another observation was the formation a thin layer of solid at the base of the glass vial. Similar drug phase separation was also observed by Westesen and co-workers during their study on the stability of phospholipid / tyloxapol trimyristin, Witepsol H42 and Witepsol H35 nanoparticles (Westesen K et al., 1997). The authors proposed that the gel formation is due to the difference in property of the colloidal lipid emulsions and suspension, and could be prevented by the use of a co-surfactant (Westesen K et al., 1997).

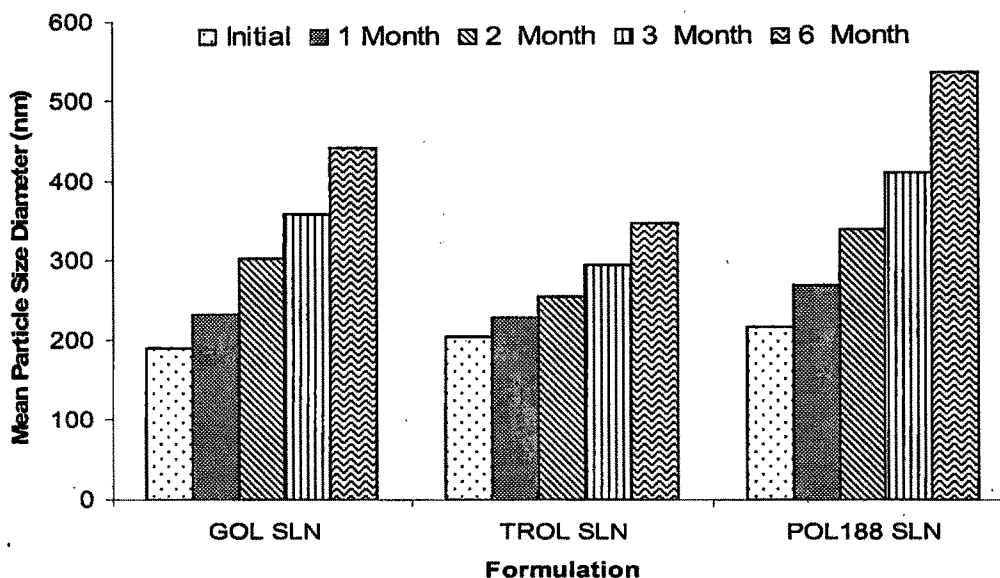


FIGURE 13.9: Mean particle diameter of the various OL loaded SLN formulations stored at 4°C after 1, 2, 3 and 6 months.

A gradual particle size growth was observed increasing storage temperatures. Increase in the storage temperature is accompanied with an increase in the input energy which would destabilize of the nanoparticle dispersion. This input energy increases the kinetic energy of the particles which leads to increased particle - particle collision and ultimately results in aggregation. Aggregation of particles may lead to the partial destruction of the protective surfactant film covering the surface of the nanoparticle. This leads to exposure of the lipid which subsequently ends in bridging the particles. The surfactant used in this study, i.e. glycol copolymers (poloxamer) are characterized with reduced aqueous solubility at higher temperatures, which can lead to particle aggregation at higher temperatures. Cleavage of hydrogen bonds between the hydrated polymer and water occurs at higher temperatures, leading to the formation of visible polymer aggregates (“cloud point”).

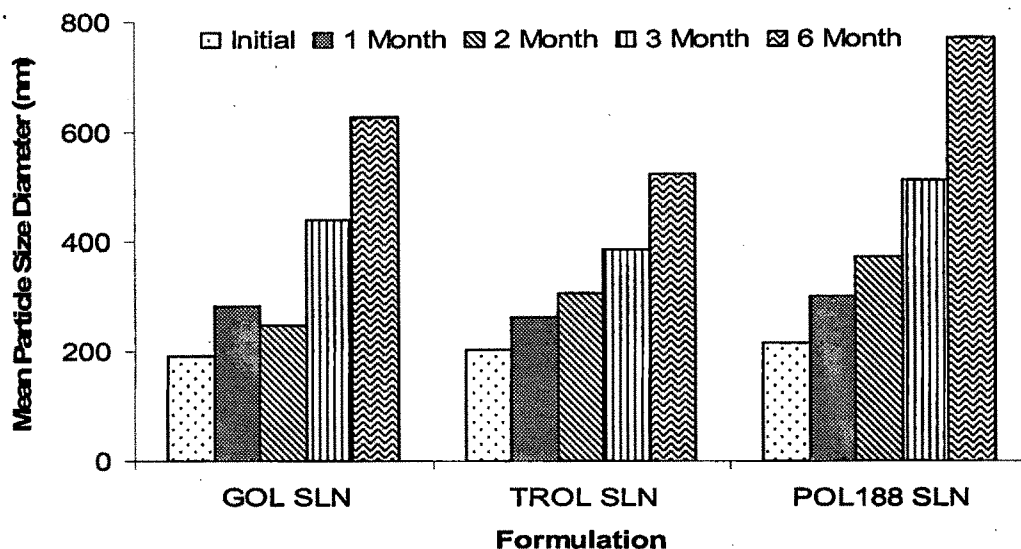


FIGURE 13.10: Mean particle diameter of the various OL loaded SLN formulations stored at 40°C after 1, 2, 3 and 6 months.

Effect of temperature on zeta potential

The zeta potential was found to drop with the increasing time duration of storage and increasing temperature. The changes in the zeta potential were more prominent for all the OL loaded SLN samples stored at 40°C (Figure 13.12) when compared with those stored at 4°C (Figure 13.11). Increase in energy input to the SLN dispersion can lead to changes in the crystalline structure of the lipid (Freitas et al., 1998). Siekmann observed an increased β -modification during the storage of tripalmitate SLN (Siekmann B and Westesen et al., 1992). Crystalline re-orientation can result in changes of the charges on the particle surface (Nernst potential) and subsequently the zeta potential. In addition, different sides of a crystal can possess different charge density (e.g. aluminium silicates like Bentone™). Formation of long β crystals can take place during one-dimensional growth of a crystal (Sato K., 1988). This ultimately results in modification in the surface ratio of differently charged crystal sides and consequently the zeta potential changes.

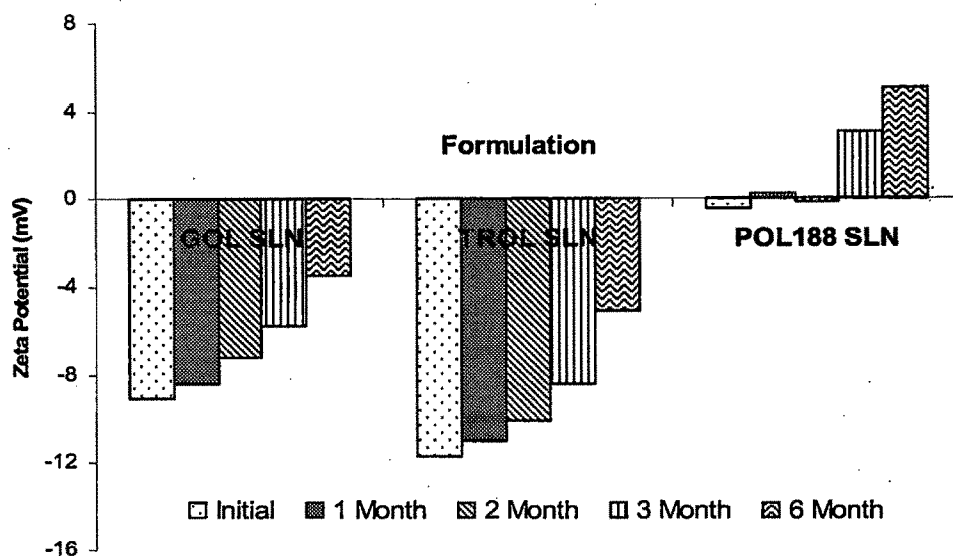


FIGURE 13.11: Zeta Potential values of the various OL loaded SLN formulations stored at 4°C after 1, 2, 3 and 6 months.

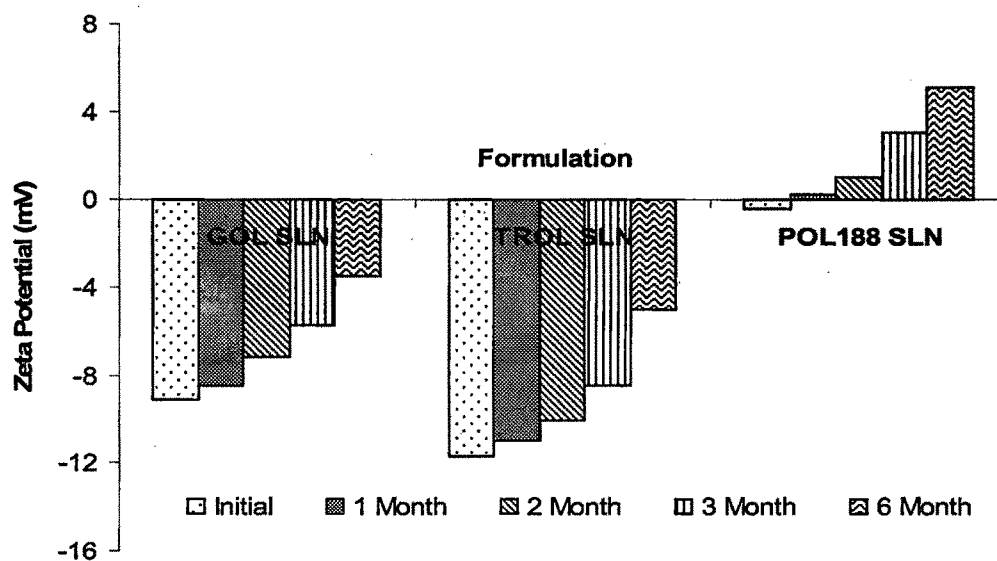


FIGURE 13.12: Zeta Potential values of the various OL loaded SLN formulations stored at 40°C after 1, 2, 3 and 6 months.

In vitro release

The release of active substances from the matrix is influenced by the crystal structure of the lipid (Lukowski G et al., 2000). In vitro release of OL from the four SLN formulations was studied in 0.1N HCl (Figure 13.13) and pH 7.4 PB (Figure 13.14). The release profiles indicated that SLN dispersions showed a retarded release of the drug from the lipid matrix. The release profiles of all the four types of SLNs best fitted into the Higuchi equation (table 13.7). Comparative $t_{25} \pm S.D$ (time taken for 25% olanzapine to be released) t_{50} values (time taken for 50% olanzapine to be released) and t_{90} (time taken for 90% olanzapine to be released) of olanzapine solution and the various nanoparticle formulations in 0.1N HCl and phosphate buffer pH 7.4 is given in table 13.8 and 13.9 respectively.

All the nanoparticles exhibited initial burst release followed by sustained release. The initial in vitro burst release is probably caused by the drug adsorbed on the nanoparticle surface or precipitated from the superficial lipid matrix (Reddy LH and Murthy RSR., 2005). The sustained release following the initial burst release is probably due to the diffusion of drug from the lipid matrix.

SLN Type	0.1N HCL		pH 7.4 PB	
	Higuchi (R^2)	Slope	Higuchi (R^2)	Slope
GOL SLN	0.9883	24.191	0.9899	11.151
TROL SLN	0.9912	24.156	0.9948	11.285
POL188 SLN	0.9907	24.474	0.9932	10.542

TABLE 13.7: Kinetic evaluation of the OL release data for the different SLN formulations in 0.1N HCL and pH 7.4 PB

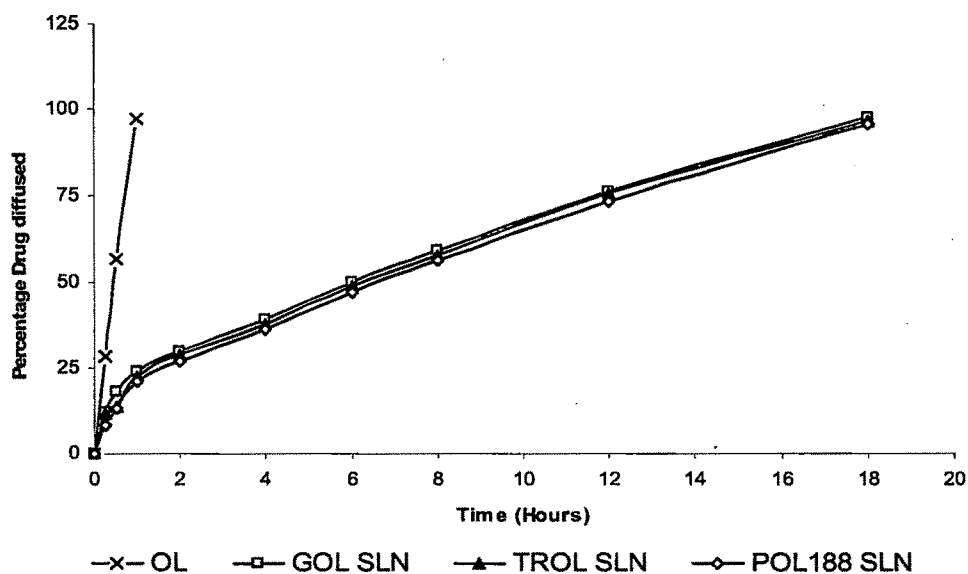


FIGURE 13.13: In vitro release of OL from plain OL solution and the various OL loaded SLN dispersions in 0.1N HCl.

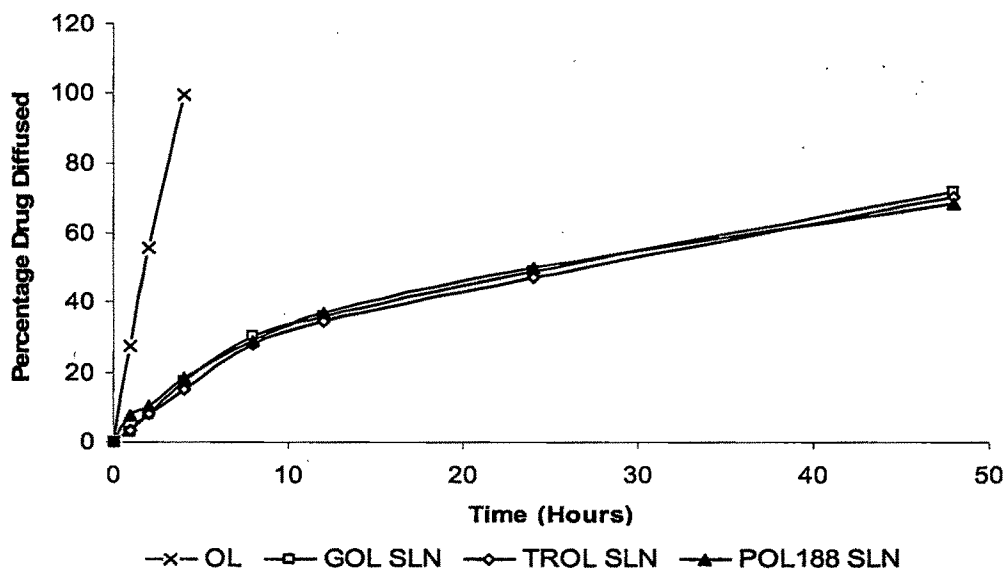


FIGURE 13.14: In vitro release of OL from plain OL solution and the various OL loaded SLN dispersions in phosphate buffer pH 7.4.

Parameter	Time in minutes			
	Plain OL Solution	GOL SLN	TROL SLN	POL188 SLN
t ₂₅	18.24 ± 1.09	65.36 ± 1.94	68.61 ± 1.22	68.12 ± 1.32
t ₅₀	35.42 ± 1.26	366.64 ± 4.97	376.72 ± 4.14	382.02 ± 4.11
t ₉₀	61.06 ± 1.44	924.69 ± 7.01	931.76 ± 6.51	942.10 ± 6.83

Table 13.8: Comparative t₂₅ ± S.D (time taken for 25% olanzapine to be released) t₅₀ values (time taken for 50% olanzapine to be released) and t₉₀ (time taken for 90% olanzapine to be released) of olanzapine solution and the various nanoparticle formulations. (Media: 0.1N HcL)

Parameter	Time in hours			
	Plain OL Solution	GOL SLN	TROL SLN	POL188 SLN
t ₂₅	1.03 ± 0.09	6.79 ± 0.12	6.86 ± 0.19	6.94 ± 0.21
t ₅₀	2.15 ± 0.11	23.95 ± 0.44	24.30 ± 0.53	24.75 ± 0.45

Table 13.9: Comparative t₂₅ ± S.D (time taken for 25% olanzapine to be released) and t₅₀ values (time taken for 50% olanzapine to be released) of olanzapine solution and the various nanoparticle formulations. (Media: phosphate buffer pH 7.4)

13.4 CONCLUSIONS

The particle size of the nanoparticles can be controlled by varying process variables such as homogenization pressure and cycle number, and formulation variables, such as surfactant. Particle Size growth was observed when the nanoparticles were stored in the dispersion state. The nanoparticles were successfully recovered in the powder form by lyophilization. The in vitro steric stability and surface hydrophobicity of the different nanoparticles stabilized with the different Pgp inhibitors, coupled with sustained release in vitro characteristics created interest for further studies into the in vivo use of these nanoparticles as long circulating carriers in blood.

13.5 REFERENCES

- Bunjes H, Westesen K, Koch MHJ, Crystallization tendency and polymorphic transitions in triglyceride nanoparticles, *Int J Pharm.*, 1996, 129, 159–173.
- Carstensen H, Muller BW, Muller RH, Adsorption of ethoxylated surfactants on nanoparticles. I. Characterization by hydrophobic interaction chromatography, *Int J Pharm.*, 1991, 67, 29-37.
- Cavalli R, Gasco MR, Morel S, Behaviour of timolol incorporated in lipospheres in the presence of a series of phosphate esters, *STP Pharma Sci.*, 1992, 2, 514–518.
- Freitas C, Muller RH, Effect of light and temperature on zeta potential and physical stability in solid lipid nanoparticle (SLN™) dispersions, *Int J Pharm.*, 1998, 168, 221–229.
- Gessner A, Waicz R, Lieske A, Muller RH, Nanoparticles with decreasing surface hydrophobicities: influence on plasma protein adsorption, *Int J Pharm.*, 2000, 196, 245–249.
- Hamdani J, Moes AJ, Amighi K, Physical and thermal characterisation of Precirol and Compritol as lipophilic glycerides used for the preparation of controlled-release matrix pellets, *Int J Pharm*, 2003, 260,47-57.
- Heiati H, Tawashi R, Phillips NC, Drug retention and stability of solid lipid nanoparticles containing azidothymidine palmitate after autoclaving, storage and lyophilization, *J Microencapsul.*, 1998, 15, 173–184.
- Huang SK, Martin FJ, Jay G, Extravasation and transcytosis of liposomes in Kaposi's sarcoma – like dermal lesions of transgenic mice bearing HIV Tat gene, *Am J Pathol.*, 1993, 143, 10-14.
- Jenning V, Gohla S, Comparison of wax and glyceride solid lipid nanoparticles (SLN®), *Int J of Pharm.* 2000, 219–222.
- Lukowski G, Kasbohm J, Pfliegel P, Crystallographic investigation of cetylpalmitate solid lipid nanoparticles, *Int J Pharm.* 2000, 196, 201–205.
- Mehnert W, Mader K, Solid lipid nanoparticles Production, characterization and applications, *Adv Drug Del Rev.*, 2001, 47, 165–196.
- Muller RH, Keck CM, Challenges and solutions for the delivery of biotech drugs – a review of drug nanocrystal technology and lipid nanoparticles, *J Biotechnology*, 2004, 113, 151–170.

Muller RH, Mader K, Gohla S, Solid lipid nanoparticles (SLN) for controlled drug delivery - a review of the state of the art, *Eur J Pharm Biopharm.*, 2000, 50, 161-177.

Muller RH, Radtke M, Wissing SA, Nanostructured lipid matrices for improved microencapsulation of drugs, *Int J Pharm.* 2002, 121-128.

Reddy LH, Murthy RSR, Etoposide-Loaded Nanoparticles Made from Glyceride Lipids: Formulation, Characterization, in Vitro Drug Release, and Stability Evaluation, *AAPS PharmSciTech*, 2005, 6 (2) Article 24. Available at: <http://www.aapspharmscitech.org>

Sato K, Crystallization of fats and fatty acids. In: Garti N, Sato K, eds. Crystallization and Polymorphism of Fats and Fatty Acids. New York: Marcel Dekker; 1988: 227-266

Siekmann B, Westesen K, Submicron-sized parenteral carrier systems based on solid lipids, *Pharm Pharmacol Lett.*, 1992, 1, 123-126.

Subramanian N, Murthy RSR, Use of electrolyte induced flocculation technique for an in vitro steric stability study of steric study of steric stabilized liposome formulations, *Pharmazie*, 2003, 59, 74-76.

Westesen K, Bunjes H, Koch MHJ, Physicochemical characterization of lipid nanoparticles and evaluation of their drug loading and sustained release potential, *J Cont Rel.*, 1997, 48, 223-236.